# AJNR

## MRI Patterns in Pediatric CNS Hemophagocytic Lymphohistiocytosis

P. Malik, L. Antonini, P. Mannam, F.N. Aboobacker, A. Merve, K. Gilmour, K. Rao, S. Kumar, S.E. Mani, D. Eleftheriou, A. Rao, C. Hemingway, S.V. Sudhakar, J. Bartram and K. Mankad

# MRI Patterns in Pediatric CNS Hemophagocytic Lymphohistiocytosis

P. Malik, L. Antonini, P. Mannam, F.N. Aboobacker, A. Merve, K. Gilmour, K. Rao, S. Kumar, S.E. Mani, D. Eleftheriou, A. Rao, C. Hemingway, S.V. Sudhakar, J. Bartram, and K. Mankad

## ABSTRACT

**BACKGROUND AND PURPOSE:** Neuroimaging has an important role in detecting CNS involvement in children with systemic or CNS isolated hemophagocytic lymphohistiocytosis. We characterized a cohort of pediatric patients with CNS hemophagocytic lymphohistiocytosis focusing on neuroradiologic features and assessed whether distinct MR imaging patterns and genotype correlations can be recognized.

**MATERIALS AND METHODS:** We retrospectively enrolled consecutive pediatric patients diagnosed with hemophagocytic lymphohistiocytosis with CNS involvement treated at 2 pediatric neurology centers between 2010 and 2018. Clinical and MR imaging data were analyzed.

**RESULTS:** Fifty-seven children (40 primary, 70%) with a median age of 36 months (interquartile range, 5.5–80.8 months) were included. One hundred twenty-three MR imaging studies were assessed, and 2 broad imaging patterns were identified. Pattern 1 (significant parenchymal disease, 32/57, 56%) was seen in older children ($P = .004$) with worse clinical profiles. It had 3 onset sub-patterns: multifocal white matter lesions (21/32, 66%), brainstem predominant disease (5, 15%), and cerebellitis (6, 19%). All patients with the brainstem pattern failed to meet the radiologic criteria for chronic lymphocytic inflammation with pontine perivascular enhancement responsive to steroids. An attenuated imaging phenotype (pattern 2) was seen in 25 patients (44%, 30 studies) and was associated with younger age.

**CONCLUSIONS:** Distinct MR imaging patterns correlating with clinical phenotypes and possible genetic underpinnings were recognized in this cohort of pediatric CNS hemophagocytic lymphohistiocytosis. Disruptive mutations and missense mutations with absent protein expression correlate with a younger onset age. Children with brainstem and cerebellitis patterns and a negative etiologic work-up require directed assessment for CNS hemophagocytic lymphohistiocytosis.

**ABBREVIATIONS:** CLIPPERS = chronic lymphocytic inflammation with pontine perivascular enhancement responsive to steroids; HLH = hemophagocytic lymphohistiocytosis; HSCT = hematopoietic stem cell transplant

Recent developments in our understanding of the underlying molecular mechanisms of degranulation defects have revealed hemophagocytic lymphohistiocytosis (HLH) to be a markedly heterogeneous disorder in which there is toxic uncontrolled immune activation. This is often driven by genetic mutations occurring along the perforin-dependent granule exocytosis pathway, termed "primary HLH."[1] Systemic inflammation and immunotherapies may also cause macrophage activation, frequently in the absence of these genetic mutations, termed "secondary HLH."

MR imaging in CNS HLH is a helpful adjunct in diagnosis but does not form a part of the HLH-2004 diagnostic criteria (https://onlinelibrary.wiley.com/doi/10.1002/pbc.21039). However, children with CNS-restricted HLH or in whom CNS HLH precedes systemic involvement often do not satisfy these criteria and have normal blood counts and systemic inflammatory markers.[2] MR imaging findings in these children overlap with infections, demyelination, and other neuroinflammatory disorders, leading to a delayed diagnosis, thus affecting outcomes. Reports of potentially distinct

Please address correspondence to Kshitij Mankad, MD, Pediatric Neuroradiology unit, Great Ormond St Hospital for Children, Great Ormond St, London WC1N 3JH, UK; e-mail: drmankad@gmail.com; @PrateekM77; @drmankad; @SSudhakar2019

neuroimaging patterns exist in the literature.[2,3] However, their incidence, clinical and genotype correlations, and impact on outcomes remain unexplored.

We present clinical profiles, MR imaging findings, and outcomes in a large pediatric cohort of HLH with CNS involvement with the aim to define distinct MR imaging patterns and correlate these with clinical profiles and explore possible genotype correlations.

## MATERIALS AND METHODS

This retrospective cohort study recruited children with HLH and CNS involvement presenting to Christian Medical College, Vellore, India, and Great Ormond Street Hospital for Children, London, UK, between 2010 and 2018. Institutional review boards from both centers approved the study. The diagnosis of HLH was defined using the HLH-2004 criteria (https://onlinelibrary.wiley.com/doi/10.1002/pbc.21039),[4] and patients with both primary and secondary HLH were included. The definition of CNS involvement was based on the presence of CSF abnormalities (proteinosis and/or pleocytosis) with or without neurologic symptoms or imaging findings.[4] Children who satisfied the above criteria with available MR images were included for data collection. Children with systemic HLH without CNS involvement based on the above definition or no available MR imaging were excluded from the study.

Demographic, clinical, and outcome data were reviewed. Imaging data collection and pattern allocation (Online Supplemental Data), blinded to the clinical data, was performed by trained neuroradiologists (P.M., S.V.S., with 5–15 years' experience) on separate MR imaging data-collection sheets with consensus agreement. Any disagreement was resolved by a consensus review with a third neuroradiologist (K.M., with 15 years' experience). The supratentorial and infratentorial compartments were further separately assessed for lesion number (single, few, multiple), lesion type (diffuse or focal), level of white matter involvement (subcortical, deep, periventricular), signal characteristics (T2WI/FLAIR, DWI, and T1 postcontrast enhancement), and overall imaging pattern (pattern definitions are elaborated under Results). Flow cytometry data regarding protein expression (NK cell perforin expression and cytotoxic lymphocyte degranulation expression) were also collected and analyzed.

### MR Imaging Lesion Definitions

MR imaging was performed on a 1.5T (Magnetom Avanto; Siemens) or a 3T (Intera Achieva; Philips Healthcare) scanner. Signal characteristics were assessed on spin-echo T2WI or FLAIR spin-echo, T1WI, T1 postcontrast, and DWI sequences. They were designated T2 or FLAIR hyperintense when the signal was more than that of normal gray matter, and as T1- and T2-hypointense when it followed the signal or was darker than the signal of gray matter.[5,6]

Diffuse and focal lesions were defined as any lesion involving the gray or white matter measuring ≥2 and <2 cm, respectively.[7] Some focal lesions had T2/FLAIR hypointensity and were further characterized as "target lesions" or "target variants" on the basis of T2/FLAIR and contrast characteristics. In target lesions, the T2 hypointense component formed a middle rim separating central and peripheral T2 hyperintense areas, giving target lesions a trilaminar appearance. In target variants, the hypointense component was present in the central core of the lesion and was surrounded by hyperintense signal. Target lesions with enhancing middle rims formed the ring-enhancing lesions.

Focal patterns of enhancement were termed "nodular" when the enhancing component measured <10 mm and "homogeneous" when ≥10 mm.[8] The perivascular enhancement pattern was defined as small continuous or near-continuous punctate (<3 mm) to nodular (<10 mm) foci of enhancement often merging[8] or heterogeneous/unclassifiable if they did not satisfy the above definitions.

### Statistical Analysis

Data from the collected variables were assessed for normality using the Shapiro-Wilk test. Means for normally distributed data were compared using the Student $t$ test, while the Mann-Whitney $U$ test was used for comparing non-normally distributed unpaired groups. The $\chi^2$ and Fisher exact tests were used for analysis of categoric data when necessary. All statistical tests were 2-sided, and statistical significance was assumed at $P$ value of <.05. SPSS Version 25 software package (IBM) was used for the analysis.

## RESULTS

Fifty-seven patients satisfied the inclusion criteria. The median age of onset was 36 months with no sex predilection. Neurologic symptoms were reported in 45 patients (79%) (Table 1); seizures and encephalopathy were most common. Of the patients with neurologic symptoms, 27/45 (60%) presented with systemic disease, and 18/45 (40%) following systemic involvement. CSF data was available for 50/57 patients (88%), and 84% ($n = 42$) showed abnormalities, with CSF proteinosis (>45mg/dL) being the most common (64%). In 12 patients (21%), CSF abnormalities, either pleocytosis or proteinosis, were present with no neurologic symptoms or only mild irritability. Thirty-five (61%) patients received either HLH-1994 (etoposide, dexamethasone, with cyclosporine at week 9) or the 2004 treatment protocol (early introduction of cyclosporine along with dexamethasone and etoposide).[9,10] Of the 35 children, 25 went on to receive hematopoietic stem cell transplant (HSCT). The average follow-up in our cohort was 3.7 years ([SD, 3.9]; range 0–15 years). Nineteen of 57 (32%) children died, including 4 from the HSCT group.

### Etiology

Seventy percent ($n = 40$) of the patients had primary HLH, with a pathogenic genetic mutation identified in 31. *PRF1* (familial HLH-2) and *UNC13D* (familial HLH-3) mutations were the most common genetic defects, seen in 35% (14) and 20% (8), respectively. Of these 31 patients, data regarding genetic variants were available for 25 patients (Online Supplemental Data). Within these 25 patients, 35 genetic variants were identified. Compound heterozygous (11/25, 44%) and homozygous (11/25, 44%) mutations were nearly equally present, while monoallelic/hemizygous mutations were rare ($n = 3$). Missense (12/17, 71%) and frameshift (8/12, 67%) mutations were the most common in FHLH2 and FHLH3, respectively. In the secondary HLH cohort ($n = 17$),

**Table 1: Clinical, treatment, and outcome profiles**[a]

| Profiles | |
|---|---|
| Age | |
| Age at onset (median) (IQR) (mo) | 36 (5.5–80.8) |
| Age at CNS presentation (median) (IQR) (mo) | 49.2 (11–96) |
| Male/female (ratio) | 34:23 (1.4:1) |
| General symptoms | |
| Fever | 45/56 (80) |
| Hepato-/splenomegaly | 46/56 (82) |
| Abdominal distension | 14/56 (25) |
| CNS symptoms | 45/57, 79% |
| Seizures | 28 (62) |
| Decreased sensorium | 22 (49) |
| Meningismus | 13 (29) |
| Gait ataxia | 12 (27) |
| Hypotonia | 11 (24) |
| Minimal symptoms (mild irritability) or clinically silent patients (no symptoms with CSF abnormalities) | 12 (21) |
| CSF findings | |
| CSF analyzed at presentation | 50/57 (87) |
| Abnormal CSF | 42/50 (84) |
| CSF pleocytosis (>10 leucocytes/$\mu$L) | 25/50 (50) |
| CSF proteinosis (>45 mg/dL) | 32/50 (64) |
| Treatment | |
| HLH 1994/2004 | 35/57 (61) |
| IT methotrexate | 17 (30) |
| HSCT | 25 (45) |
| Outcome profiles | |
| Death | 19 (32) |
| Death before 8 weeks | 7 |
| Death after 8 weeks | 12 |
| Alive at last follow-up | 36 (63) |
| Lost to follow-up | 2 |

**Note:**—IQR indicates interquartile range; IT, intrathecal.

[a] Total (*n* = 57). Data collected are both continuous and categorical, and the analysis method used has been referred to under statistical analysis heading.

infections (10, 59%) and autoimmune etiologies (6, 35%) were the most common.

### Imaging Pattern Definitions

We reviewed 123 MR imaging studies from the 57 included patients. On the basis of a pattern-recognition approach, 2 broad imaging patterns were defined (pattern 1 and pattern 2).

Pattern 1, the significant parenchymal disease group, consisted of patients with parenchymal lesions. 93/123 studies (76% of studies; 32/57 patients, 56%) were grouped under pattern 1. The supratentorial and infratentorial compartments were further separately assessed for lesion number, signal, and enhancement characteristics.

Pattern 2 had an attenuated imaging phenotype with no parenchymal lesions at onset and follow-up (if available) and had nonspecific MR imaging findings, isolated cortical atrophy, or normal imaging findings.

Thirty of 123 (24% of studies; 25/57 patients, 44%) studies belonged to pattern 2. These included 10 studies with normal findings, 15 studies with only cerebral atrophy with or without cerebellar atrophy, 3 studies with central tegmental tract T2-hyperintensity as an isolated finding, 2 studies with nonspecific findings (small pons, underopercularization, germinal matrix

cysts, and periventricular hemosiderin staining attributable to a remote or perinatal event).

### Imaging Findings in Pattern 1

**Lesion Type Incidence and Distribution.** A near-equal incidence of cerebral and cerebellar involvement was seen, 77/123 (63%) and 71/123 (58%), respectively (Online Supplemental Data). Deep gray nuclear and thalamic involvement was seen in 35/123 studies (28%) and was commonly bilateral and asymmetric (24/35, 68%). Brainstem involvement with a predilection for the dorsal pons was seen in 34/123 (28%), variably extending to involve the midbrain (32/34 studies) and medulla (9/34 studies). Cranial nerve involvement was seen as bilateral nodular enhancement involving multiple nerves in 5 studies. Severe optic nerve swelling, enhancement, and diffusion restriction (Online Supplemental Data) were noted in one. Short-segment enhancing cord lesions were seen in 3 studies, along with cauda equina thickening in one.

**Enhancement Characteristics.** Enhancement was present in more than half of the studies with cerebral and cerebellar lesions, 52% and 60%, respectively. Both the diffuse (77%) and focal (80%) cerebellar lesions showed a higher proportion of enhancement than their cerebral counterparts (26%, 60%, respectively). Diffuse lesions showed a perivascular pattern of enhancement most commonly, while focal lesions most commonly showed nodular/homogeneous enhancement. Target lesion and target variants were seen in 6 studies with supratentorial lesions and 4 studies with infratentorial lesions. None of the target lesions or variants showed diffusion restriction.

**Other Findings.** Thirty-two of 123 studies had cortical atrophy along with parenchymal lesions. Eighteen studies showed blooming on SWI within the white matter lesions, representing either microhemorrhages or calcifications. Nineteen studies had ventriculomegaly, which was obstructive due to cerebellar edema in 3.

### Subpatterns in Pattern 1

Three onset subpatterns were identified within pattern 1 using an algorithmic approach (Online Supplemental Data) and were divided and assigned to 3 subgroups, 1.1, 1.2, and 1.3.

**Subgroup 1.1: Multifocal Cerebral/Cerebellar White Matter Lesions.** Patients in subgroup 1.1 showed involvement of cerebral and cerebellar white matter with variable numbers and signal characteristics of the lesions. This subpattern was the most common, identified in 21/32 patients (66%) at onset (Online Supplemental Data). On follow-up, this was again the largest subpattern (21, 37%), with 2 patients of subpattern 1.2 and 4 of subpattern 1.3 evolving into subpattern 1.1.

**Subgroup 1.2: Brainstem Predominant Lesions.** Subgroup 1.2 pattern was defined as numerous (>3) punctate to nodular enhancing lesions involving the pons with variable extension into the cerebellum, mesencephalon, and deep cerebral white matter and was reminiscent of the radiologic pattern seen in chronic lymphocytic inflammation with pontine perivascular enhancement responsive to steroids (CLIPPERS).[11] These were further assessed for radiologic criteria proposed for CLIPPERS, including the size of the largest T1-enhancing nodule, T2 signal extension beyond
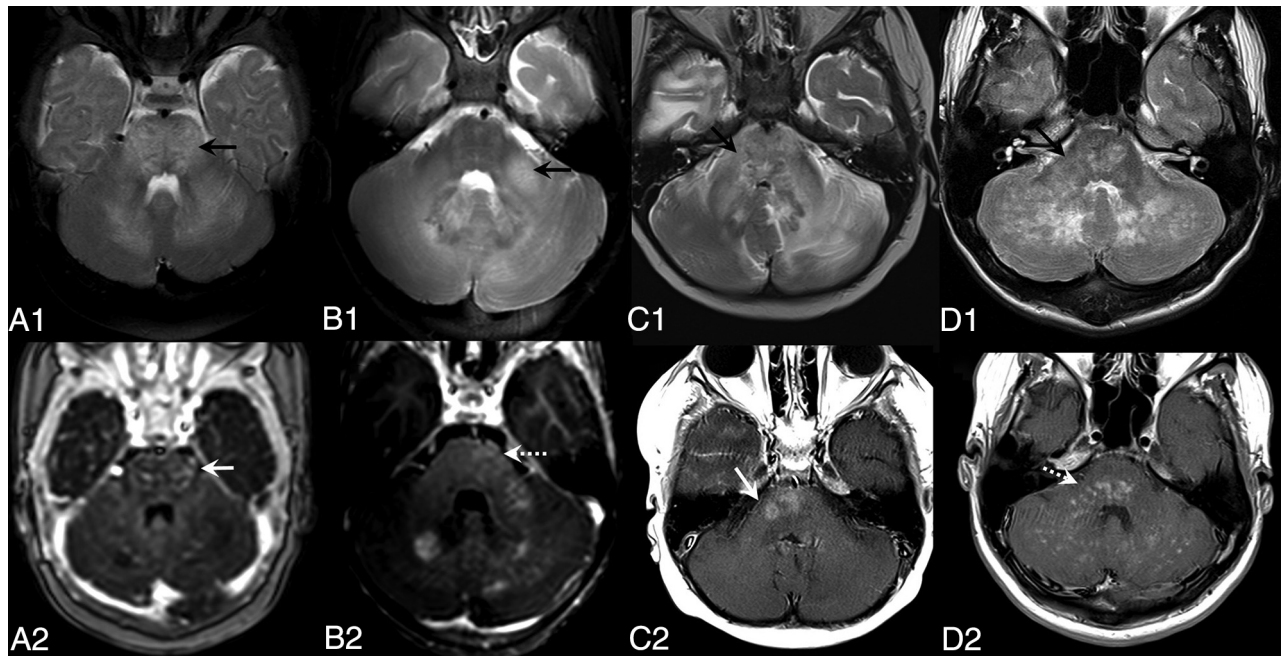
**FIG 1.** Findings of 4 patients with subpattern 1.2 (brainstem–predominant pattern). Axial T2WI (*A1–D1*) and axial postcontrast T1WI (*A2–D2*) at the level of the pons show multiple punctate (*dashed white arrow, B2, D2*) to nodular (*solid white arrow, A2 and C2*), enhancing foci and extension of the T2 signal abnormality (*black arrow, A1–D1*) beyond the enhancement in all cases.

the T1 enhancing nodule (T2-T1 mismatch), and symmetric or asymmetric involvement of the pons.[12]

This subpattern was seen in 5/32 patients (15%) at the onset of CNS HLH (Online Supplemental Data). In 1 additional patient (patient 47), this pattern was noted on follow-up with the preceding studies showing multifocal white matter lesions. In 2 of these 6 patients, CNS involvement preceded or was within 2 weeks of systemic HLH onset. The underlying genetic defect was variable. Clinically, all had signs of brainstem and/or cerebellar dysfunction along with a variable presence of encephalopathy and seizures. T2 signal abnormality always extended beyond the enhancing nodule (6/6), and in almost all (5/6), the size of the largest T1-enhancing nodule was >3 mm. Four of 6 patients showed an asymmetric involvement of the pons at the middle cerebellar peduncle level (Fig 1). Four of 6 children died (3 received an HLH therapy protocol; one received a steroid-based regimen, and one also received HSCT). For 4 patients, a follow-up imaging was available, and 3/4 developed multifocal white matter lesions.

Representative cerebellar biopsy (patient 57, Online Supplemental Data), obtained before a genetic diagnosis, showed chronic inflammation and nonspecific histologic changes.

Subgroup 1.3: Diffuse Cerebellar Involvement/Cerebellitis. Subgroup 1.3 pattern was defined as diffuse cerebellar cortical swelling/edema with diffuse effacement of cerebellar folia, with or without cerebellar white matter signal change (Fig 2). Mass effect in the form of tonsillar descent, fourth ventricular outflow obstruction, and hydrocephalus was assessed additionally.

This subpattern was seen in 6/32 patients at onset (19%, summarized in the Online Supplemental Data). In these patients, there was diffuse cerebellar edema and effacement of cerebellar folia and/or cerebellopontine cisterns. This was often severe

enough to be associated with tonsillar descent (5/6) and proximal hydrocephalus (3/6). In 4/6 children, this was the first manifestation of HLH and preceded systemic involvement. Cerebellitis was the only finding in most, barring 2 children in whom additional white matter lesions were also present. Clinically, all had signs of cerebellar dysfunction and varying degrees of encephalopathy and seizures. The cerebellar edema responded to steroids in all children. Two children had recurrent episodes of cerebellitis. *PRF1* and *UNC13D* mutations were present in 2 patients each. On follow-up, cerebellar edema resolved and evolved into multifocal white matter lesions in all.

### Pattern Analysis for Clinicoradiologic Correlation
Patterns 1 and 2, along with the subpatterns, were assessed for clinical and outcome differences. Children with pattern 1 were significantly older (median age, 55.5 versus 16 months, *P* value = .004) and had a worse symptom profile for most symptoms (Table 2). Both patterns 1 and 2 had a high incidence of CSF abnormalities (90% and 75%, respectively); significant pleocytosis was noted in pattern 1 (*P* value = .04). Pattern 1 was associated with nearly twice the incidence of mortality and a lower deficit-free survival, though this was not statistically significant (*P* value = .06). These parameters were not statistically different across the subpatterns.

### Genotype Correlations
To analyze possible genotype correlations, we pooled patients with at least 1 disruptive mutation (nonsense, frameshift, or deletion) and missense mutations with absent protein expression together (pooled mutation group) and compared them against children with missense mutations and residual protein expression (Online Supplemental Data). We also assessed the purely disruptive mutation group separately for the same variables.
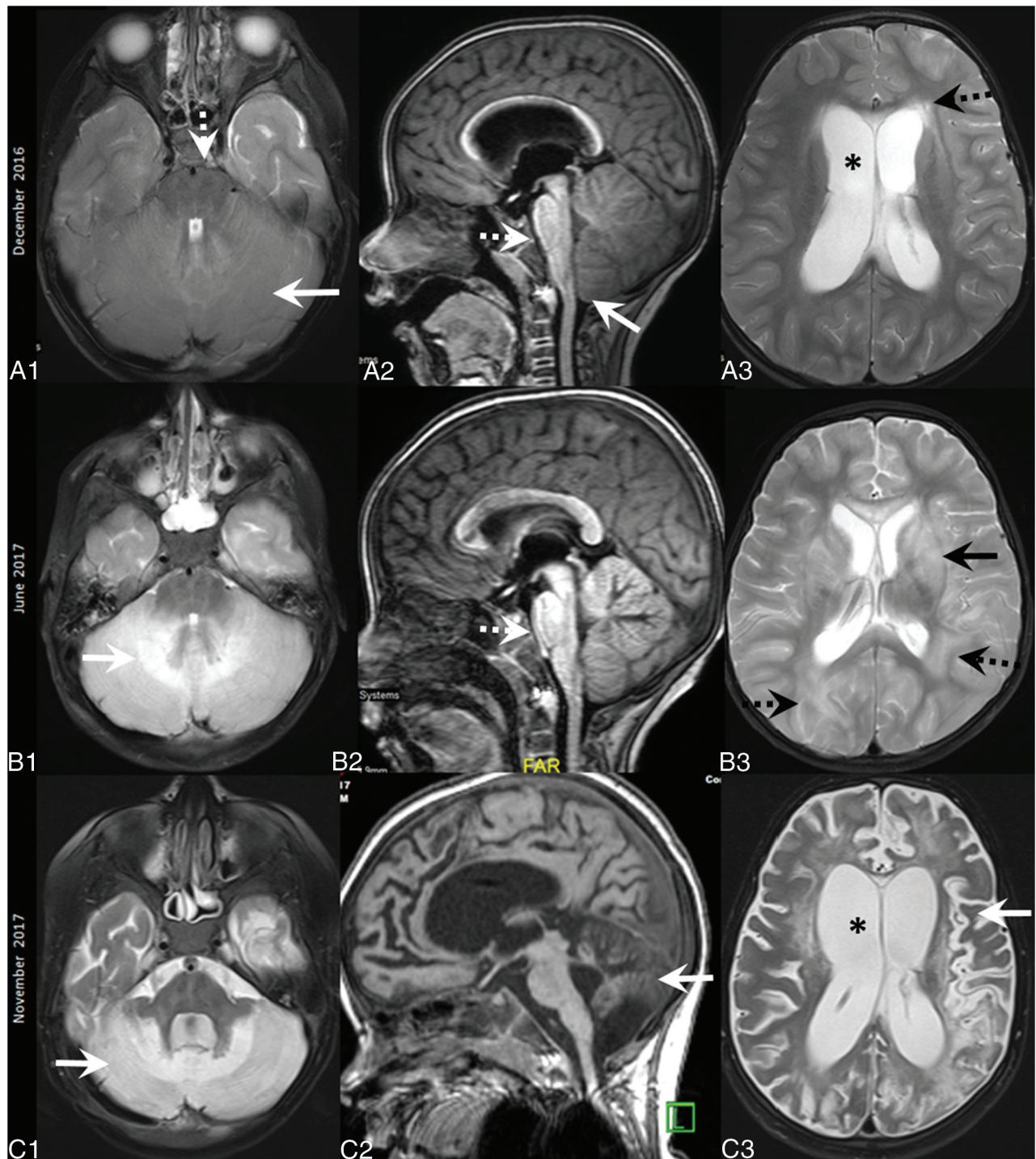
**FIG 2.** Findings of subpattern 1.3 (cerebellitis). Axial T2WI at the level of the fourth ventricle (*A1–C1*), lateral ventricles (*A3–C3*), and midline sagittal T1WI (*A2–C2*). Onset MR imaging (December 2016) shows severe cerebellar edema and expansion (*white arrow, A1*) with mass effect on the brainstem, effacement of the prepontine cistern (*dashed white arrow, A2*), and foramen magnum crowding (*white arrow, A2*). Lateral ventricular dilation (*asterisk, A3*) and transependymal CSF seepage (*dashed black arrow, A3*) are also noted. Mild reduction in cerebellar edema and mass effect (*dashed arrow, B2*) with new cerebellar (*white arrow, B1*), parieto-occipital (*dashed arrow, B3*), and deep gray nuclei (*black arrow, B3*) hyperintensities were found in June 2017. Last MR imaging in November 2017 shows cerebral (*white arrow, C3*) and cerebellar (*white arrows, C1–2*) atrophy, diffuse white matter hyperintensities, and ventriculomegaly (*asterisk, C3*).

The age of onset of disease was significantly younger in the purely disruptive mutation group (median age, 3 versus 20 months in children without purely disruptive mutations, *P* value = .03) and in the pooled mutation group (median age, 4.7 versus 74.4 months

in children with missense mutations with residual protein expression, *P* value = .03). A higher proportion of patients with pattern 2 belonged to the pooled mutation group (13/13) in comparison with pattern 1 (9/12, 75%), with trends toward significance (*P*

**Table 2: Pattern characteristics and analysis**[a]

| | Subpatterns | | | P Value | Pattern 1 Overall | Pattern 2 | P Value |
|---|---|---|---|---|---|---|---|
| | 1.1 | 1.2 | 1.3 | | | | |
| Median age at onset (mo) | 45.4 | 66 | 80.5 | .5 | 55.5 | 16 | .004 |
| Symptoms | | | | | | | |
|   Seizures | 11/21 (52%) | 4/5 (80%) | 4/6 (67%) | .5 | 19/32 (59%) | 9/25 (36%) | .08 |
|   Encephalopathy | 11/21 (52%) | 1/5 (20%) | 4/6 (67%) | .3 | 16/32 (50%) | 6/25 (24%) | .04 |
|   Gait ataxia | 5/21 (24%) | 3/5 (60%) | 3/6 (50%) | .08 | 12/32 (34%) | 0 | .001 |
|   Limb weakness | 6/21 (29%) | 1/5 (20%) | 1/6 (17%) | .8 | 8/32 (25%) | 1/25 (4%) | .03 |
|   Dysarthria | 0 | 2/5 (40%) | 1/6 (17%) | .01 | 3/32 (9%) | 1/25 (4%) | .4 |
|   Diplopia | 01/21 (5%) | 2/5 (40%) | 2/6 (33%) | .06 | 5/32 (16%) | 0 | .03 |
| Abnormal CSF | 18/20 (90%) | 4/5 (80%) | 5/5 (100%) | .6 | 27/30 (90%) | 15/20(75%) | .2 |
| Proteinosis | 13 (65%) | 4 (80%) | 4 (80%) | .5 | 21 (70%) | 11 (55%) | .3 |
| Pleocytosis | 10 (50%) | 4 (80%) | 5 (100%) | .08 | 19 (63%) | 6 (30%) | .04 |
| Pooled mutation group | 4/6 (67%) | 2/3 (67%) | 3/3 (100%) | .32 | 9/12 (75%) | 13/13 (100%) | .09 |
| Mortality | 9/20 (45%) | 3/5 (60%) | 2/6 (33%) | .3 | 14/31 (45%) | 5/24 (21%) | .06 |
| Deficit-free at follow-up | 8/20 (40%) | 1/5 (20%) | 1/6 (17%) | .1 | 10/31 (32%) | 13/25(52%) | .06 |

[a] Data collected are both continuous and categorical, and the analysis method used has been referred to under statistical analysis heading.

value = .09, Table 2). After an age-based subpattern analysis (Online Supplemental Data), we further noted that patients in the pooled mutation group who presented after 12 months had either posterior fossa patterns 1.2 and 1.3 or pattern 2 (3/6 each). All children with missense mutations with residual protein expression presented after 12 months of age with pattern 1.1 (3/3).

All recurrent mutations in our cohort belonged to the pooled mutation group (Online Supplemental Data) with predominance of pattern 2 except c.50del(p.Leu17Argfs*34, which also had patterns 1.1 and 1.3.

## DISCUSSION

CNS HLH, a genetically heterogeneous entity, is neuroradiologically characterized by multifocal parenchymal lesions and atrophy as its most common manifestations. Anecdotal evidence suggests that atypical MR imaging patterns exist; however, these remain unexplored in larger cohort studies. Through our retrospective cohort study, we describe 2 broad MR imaging patterns comprising parenchymal lesions (pattern 1, 32/57 patients, 56%) and an attenuated phenotype with normal-to-nonspecific findings (pattern 2, 25/57 patients; 44%). The attenuated phenotype (pattern 2) affected younger children (16 months, P value = .004), had a better symptom profile and a higher deficit-free survival (52%, P value = .06). Significant parenchymal disease (pattern 1) was more common in older children (55.5 months) and had 3 distinct imaging subpatterns at onset: multifocal white matter lesions (21/32, 66%), a brainstem–predominant pattern (5/32, 15%), and cerebellitis (6/32, 19%). We summarize their radiologic features, evolution and highlight possible genotype correlations related to these patterns.

CNS involvement in HLH is an independent, poor prognostic factor in children and is associated with significant morbidity and mortality.[13,14] A consensus agreement on a standardized definition of CNS HLH in the literature is lacking, and variable importance has been attached to clinical and imaging findings.[4,15,16] Previous studies have stressed the importance of rigorously evaluating clinical, CSF, and MR imaging findings in assessing CNS involvement.[17] Because MR imaging findings can precede clinical and CSF abnormalities,[17] we used a comprehensive definition,

including CSF, clinical, and imaging findings.[4,18] Imaging findings are highly variable, ranging from normal, isolated cortical atrophy to parenchymal lesions. Cortical atrophy is common in CNS HLH[16,17,19] but must be viewed with caution when present in isolation, especially in the background of steroid administration.[17] To address this issue, we used a pattern-recognition approach and segregated the parenchymal lesion group (pattern 1) from patients with nonspecific findings, normal imaging, and isolated cortical atrophy (pattern 2).

Consistent with previous studies, multifocal white matter lesions were the most common finding,[5,20] and frequent cerebral and cerebellar involvement was noted. Multifocal lesions, tumefactive lesions, optic neuritis, and spinal cord lesions can be seen in CNS HLH and overlap with pediatric acquired demyelinating syndromes and infiltrative disorders.[21] While distinct clinicoradiologic syndromes have been described in acquired demyelinating syndromes,[21] such phenotypes remain elusive in CNS HLH. We identified 3 distinct MR imaging subpatterns, 2 of which were seen in children with an acute-to-subacute brainstem and/or cerebellar dysfunction. These subpatterns include multifocal white matter lesions, brainstem–predominant disease, and cerebellitis.

CLIPPERS, a steroid-responsive immune-mediated predominant T-cell perivascular brainstem infiltrative process, has been described mainly in the adult population, and its distinct brainstem radiologic pattern enables identification in the presence of typical features.[8,11] In 2017, clinical, radiologic and pathologic diagnostic criteria were proposed to distinguish CLIPPERS from its mimics,[12] which have been validated in few subsequent studies.[8] Systematic studies evaluating CLIPPERS in pediatric cohorts, however, remain lacking due to differences in disease burden. There is increasing evidence to suggest that unlike in adults, children with a clinicoradiologic phenotype of CLIPPERS have a more aggressive clinical course and higher disability scores on follow-up.[22,23] Pediatric CNS HLH resembling CLIPPERS has been described in the literature (Table 3)[2,24]; however, the radiologic criteria have not been methodically explored. The brainstem–predominant pattern in our cohort was reminiscent of CLIPPERS, though there were important differences (Online Supplemental Data). None of our patients satisfied all the radiologic criteria

**Table 3: Relevant literature review of CNS HLH cases with brainstem or cerebellitis patterns with available MR imaging and genetic data**

| Literature Review | Imaging Pattern | Genetic Variants | Age of Onset, Relation to Systemic HLH | Imaging Findings |
|---|---|---|---|---|
| Benson et al[2] 3 cases | Brainstem–predominant pattern (CLIPPERS-like) | 1 disruptive, 2 with missense mutations and absent protein expression<br>Pt 1: *PRF1* c.452A>T (p.H151L) and c.666C>A (H222Q), Perforin expression 0%<br>Pt 2: *PRF1* c.443C>G (p.A148G) and c.666C>A (H222Q), Perforin expression 0%<br>Pt 3: *UNC13D* c.2346_2349delGGAG (p.R782fs), c.2588G>A (p.G863D) | 5–7 yr, all 3 CNS-restricted HLH | CLIPPERS MR imaging criteria NA |
| Taieb et al[28] 4 patients | Brainstem–predominant pattern (CLIPPERS-like) | 4 cases, all with missense mutations and retained-but-decreased protein expression<br>Pt 1: *PRF1* c.272C>T(p.A91V) homozygous, perforin expression 38%<br>Pt 2: *UNC13D* c.919C>T (p.Q307*) and c.2038C>T (p.R680W), not applicable<br>Pt 3: *PRF1* c.116C>A (p.P39H) and c.272C>T (p.A91V), perforin expression 25%<br>Pt 4: *PRF1* c.82C>T (p.R28C) and c.272C>T (p.A91V), perforin expression 38% | Adults (42–73 yr), all had CNS-restricted HLH | Three-fourths had atypical MR imaging CLIPPERS features (confluent contrast-enhancing lesions) |
| Bhoopalan et al[26] 1 patient | Cerebellitis | 1 patient with compound heterozygous *PRF1* gene mutations with at least 1 disruptive mutation *PRF1*: c.50delT (p.L17fs) and c.527G>A(p.C176Y)) | 8 yr, CNS-restricted HLH | Cerebellitis, tonsillar herniation, no multifocal lesions |
| Khan et al[27] 1 patient | Cerebellitis | 1 patient with homozygous missense mutation c. 173T > C (p.L58P) in STX11 (syntaxin 11) gene | 2 yr 7 months, systemic HLH already present | Cerebellitis, tonsillar herniation, diffuse-to-multifocal lesions already present |
| Astigarraga et al[3] 1 patient | Cerebellitis | 1 patient with compound heterozygous missense *PRF* mutations *PRF1*: c.643C>A (p.L215I) and c.785C>A (p.Ala262Asp) (perforin expression data NA) | 3 yr, preceded systemic HLH | Recurrent cerebellitis, tonsillar herniation, subsequently multifocal lesions |
| Taieb et al[28] 1 patient | Cerebellitis | Patient 3's (in CLIPPERS series) brother's; granddaughter, monoallelic *PRF1* mutation (genetic variant NA) | Not specified, self-limited CNS-restricted presentation | NA |
| Chiapparini et al[29] 1 patient | Cerebellitis | 1 patient with homozygous missense *PRF1* mutation c.673C>T (p. Arg225Trp) (perforin expression data NA) | 13 yr, preceded systemic HLH | Cerebellitis, tonsillar herniation followed by multifocal lesions |

**Note:**—NA indicates not available; Pt, patient.

for CLIPPERS, and extension of T2 signal change beyond the enhancing nodule was present in all (6/6). Nodular enhancement (5/6) and asymmetric involvement of the pons (4/6) were frequently seen as well. Demyelination work-up, including myelin oligodendrocyte glycoprotein antibody-associated disease,[25] returned negative results, and poor-to-partial responsiveness was noted in those who received steroids. While all cases in literature had CNS-restricted HLH (Table 3), in most (4/6) of our patients, systemic HLH signs were present. After a negative etiologic work-up in this brainstem pattern, CNS HLH evaluation remains imperative in children due to

differences in treatment strategies in comparison with other neuroinflammatory disorders.

We also describe 6 children in our cohort (Online Supplemental Data) with cerebellar dysfunction and diffuse cerebellar edema on MR imaging (subpattern 1.3). All children, except 1, presented with this subtype as the first CNS manifestation, and it preceded systemic HLH involvement in most (4/6). In all children, the findings of the diagnostic work-up for cerebellitis were negative, and cerebellar edema responded to steroids. Five similar children with imaging showing cerebellar swelling at the onset of primary HLH have been described previously (Table

3).[3,26-29] Cerebellitis preceded systemic involvement or was followed by CNS-restricted disease in 4 cases. An unfamiliarity with this pattern led to diagnostic delays, and these children subsequently developed multifocal white matter lesions on follow-up. Thus, cerebellar edema and cerebellar dysfunction can be the only finding at the onset of CNS HLH.

Pattern 1 had an older age of onset, worse symptomatology, and trends toward poorer outcomes. The role of hypomorphic missense mutations with residual protein expression is being increasingly recognized in late-onset HLH forms.[20,30] To understand the relationship between onset age and differential brain involvement, we explored possible genotype correlations in our cohort. Consistent with prior studies,[31] both purely disruptive and pooled mutation groups (consisting of children with at least 1 disruptive mutation or missense mutations with absent protein expression) had a younger age of onset. All patients with missense mutations with residual protein expression (hypomorphic mutations) presented after 12 months of age (3/3).

The pooled mutation group also had a higher proportion of patients with pattern 2 (100% versus 75% with pattern 1, *P* value =.09), potentially explaining the younger age of onset with this pattern. This association did not reach statistical significance (*P* value =.09), and we attribute this to the fact that some patients in the pooled mutation group indeed presented after 12 months of age. Interestingly, up to half of the patients with late-onset and disruptive mutations presented with posterior fossa patterns 1.2 and 1.3 (3/6, Online Supplemental Data). Similarly, all patients in the hypomorphic mutation group presented with the more typical pattern. 1.1 (3/3, Online Supplemental Data). We noted many similarities with cases reported in literature. All 8 children with reported MR imaging patterns 1.2 or 1.3 presented after 12 months, between 3 and 13 years of age (Table 3).[2,3,26,27,29] All patients with pattern 1.2 (3/3) had at least 1 disruptive mutation or missense mutations with absent protein expression.[2] Most patients with pattern 1.3 had either disruptive or missense mutations (4/5), but the data regarding protein expression in cases with missense mutations was not available (Table 3). The small number of genetically confirmed patients in the subgroups limits our interpretation. However, the tendency of disruptive mutations and missense mutations with absent protein expression to present with atypical brainstem or cerebellitis patterns in young children after 12 months of age requires further exploration. A CLIPPERS-like pattern has been reported in adult-onset HLH with hypomorphic missense mutations with residual protein expression.[28] This association, thus, may possibly be limited to young children, and there may be other age-related factors, extrinsic triggers, and susceptibility loci influencing MR imaging pattern presentations.

We acknowledge the inherent limitations of our study due to its retrospective nature. Standardizing MR imaging protocols during the 8-year period from which the patients' records were recruited was difficult, and imaging parameters could have differed during this period and between institutions. Interpretation of the genotype correlation analysis remains limited due to small number of patients in the subgroups.

## CONCLUSIONS

We systematically described MR imaging findings in a pediatric cohort of CNS HLH. Older children more commonly had a significant parenchymal disease pattern, which was associated with a worse clinical profile and 3 distinct subpatterns. We confirm a genotype correlation between disruptive mutations and a younger age of presentation and expand the same to an attenuated imaging pattern (pattern 2). Larger studies are needed to examine a possible age-related tendency of late-onset disruptive mutations or missense mutations with absent protein expression to present with atypical MR imaging patterns. Finally, because CNS manifestations can precede systemic signs and even remain restricted to the CNS, HLH should be considered in patients with atypical imaging presentations such as brainstem lesions or cerebellar edema and negative findings on work-up for other etiologies because this may be the only finding heralding the onset of HLH.

## REFERENCES

1. Voskoboinik I, Smyth MJ, Trapani JA. **Perforin-mediated target-cell death and immune homeostasis.** *Nat Rev Immunol* 2006;6:940–52 CrossRef Medline
2. Benson LA, Li H, Henderson LA, et al. **Pediatric CNS-isolated hemophagocytic lymphohistiocytosis.** *Neurol Neuroimmunol Neuroinflamm* 2019;6:e560 CrossRef Medline
3. Astigarraga I, Prats JM, Navajas A, et al. **Near fatal cerebellar swelling in familial hemophagocytic lymphohistiocytosis.** *Pediatr Neurol* 2004;30:361–64 CrossRef Medline
4. Koh KN, Im HJ, Chung NG, et al; Korea Histiocytosis Working Party. **Clinical features, genetics, and outcome of pediatric patients with hemophagocytic lymphohistiocytosis in Korea: report of a nationwide survey from Korea Histiocytosis Working Party.** *Eur J Haematol* 2015;94:51–59 CrossRef Medline
5. Deiva K, Mahlaoui N, Beaudonnet F, et al. **CNS involvement at the onset of primary hemophagocytic lymphohistiocytosis.** *Neurology* 2012;78:1150–56 CrossRef Medline
6. Rovaris M, Comi G, Rocca MA, et al. **Relevance of hypointense lesions on fast fluid-attenuated inversion recovery MR images as a marker of disease severity in cases of multiple sclerosis.** *AJNR Am J Neuroradiol* 1999;20:813–20 Medline
7. Mikaeloff Y, Adamsbaum C, Husson B, et al; KIDMUS Study Group on Radiology. **MRI prognostic factors for relapse after acute CNS inflammatory demyelination in childhood.** *Brain* 2004;127:1942–47 CrossRef Medline
8. Taieb G, Mulero P, Psimaras D, et al; French CLIPPERS group. **CLIPPERS and its mimics: evaluation of new criteria for the diagnosis of CLIPPERS.** *J Neurol Neurosurg Psychiatry* 2019;90:1027–38 CrossRef Medline
9. Henter JI, Samuelsson-Horne A, Aricò M, et al; Histocyte Society. **Treatment of hemophagocytic lymphohistiocytosis with HLH-94 immunochemotherapy and bone marrow transplantation.** *Blood* 2002;100:2367–73 CrossRef Medline
10. Bergsten E, Horne A, Aricó M, et al. **Confirmed efficacy of etoposide and dexamethasone in HLH treatment: long-term results of the cooperative HLH-2004 study.** *Blood* 2017;130:2728–38 CrossRef Medline
11. Pittock SJ, Debruyne J, Krecke KN, et al. **Chronic lymphocytic inflammation with pontine perivascular enhancement responsive to steroids (CLIPPERS).** *Brain* 2010;133:2626–34 CrossRef Medline
12. Tobin WO, Guo Y, Krecke KN, et al. **Diagnostic criteria for chronic lymphocytic inflammation with pontine perivascular enhancement**

responsive to steroids (CLIPPERS). *Brain* 2017;140:2415–25 CrossRef Medline

13. Xu XJ, Wang HS, Ju X-L, et al; Histiocytosis Study Group of the Chinese Pediatric Society. **Clinical presentation and outcome of pediatric patients with hemophagocytic lymphohistiocytosis in China: a retrospective multicenter study.** *Pediatr Blood Cancer* 2017;64:e26264 CrossRef Medline

14. Haddad E, Sulis ML, Jabado N, et al. **Frequency and severity of central nervous system lesions in hemophagocytic lymphohistiocytosis.** *Blood* 1997;89:794–800 Medline

15. Jovanovic A, Kuzmanovic M, Kravljanac R, et al. **Central nervous system involvement in hemophagocytic lymphohistiocytosis: a single-center experience.** *Pediatr Neurol* 2014;50:233–37 CrossRef Medline

16. Kollias SS, Ball WS, Tzika AA, et al. **Familial erythrophagocytic lymphohistiocytosis: neuroradiologic evaluation with pathologic correlation.** *Radiology* 1994;192:743–54 CrossRef Medline

17. Horne A, Trottestam H, Aricò M, Histiocyte Society, et al. **Frequency and spectrum of central nervous system involvement in 193 children with haemophagocytic lymphohistiocytosis.** *Br J Haematol* 2008;140:327–35 CrossRef Medline

18. Ma W, Li XJ, Li W, et al. **MRI findings of central nervous system involvement in children with haemophagocytic lymphohistiocytosis: correlation with clinical biochemical tests.** *Clin Radiology* 2021;76:159.e9-159–17 CrossRef Medline

19. Rego I, Severino M, Micalizzi C, et al. **Neuroradiologic findings and follow-up with magnetic resonance imaging of the genetic forms of haemophagocytic lymphohistiocytosis with CNS involvement.** *Pediatr Blood Cancer* 2012;58:810–14 CrossRef Medline

20. Blincoe A, Heeg M, Campbell PK, et al. **Neuroinflammatory disease as an isolated manifestation of hemophagocytic lymphohistiocytosis.** *J Clin Immunol* 2020;40:901–16 CrossRef Medline

21. Chhabda S, Malik P, Reddy N, et al. **Relapsing demyelinating syndromes in children: a practical review of neuroradiological mimics.** *Front Neurol* 2020;11:627 CrossRef Medline

22. Sa M, Green LM, Abdel-Mannan O, et al. **Is chronic lymphocytic inflammation with pontine perivascular enhancement responsive to steroids (CLIPPERS) in children the same condition as in adults? Developmental medicine and child neurology.** *Dev Med Child Neurol* 2019;61:490–96 CrossRef Medline

23. Taieb G, Duflos C, Renard D, et al. **Long-term outcomes of CLIPPERS (chronic lymphocytic inflammation with pontine perivascular enhancement responsive to steroids) in a consecutive series of 12 patients.** *Arch Neurol* 2012;69:847–55 CrossRef Medline

24. McCreary D, Omoyinmi E, Hong Y, et al. **Development and validation of a targeted next-generation sequencing gene panel for children with neuroinflammation.** *JAMA Netw Open* 2019;2:e1914274 CrossRef Medline

25. Symmonds M, Waters PJ, Küker W, et al. **Anti-MOG antibodies with longitudinally extensive transverse myelitis preceded by CLIPPERS.** *Neurology* 2015;84:1177–79 CrossRef Medline

26. Bhoopalan SV, Campbell PK, Bag AK, et al. **Haemophagocytic lymphohistiocytosis restricted to the central nervous system.** *Arch Dis Child* 2021;106:527 CrossRef Medline

27. Khan SG, Binmahfoodh M, Alali M, et al. **Cerebellar swelling due to familial hemophagocytic lymphohistiocytosis: an unusual presentation.** *Eur J Paediatr Neurol* 2015;19:603–06 CrossRef Medline

28. Taieb G, Kaphan E, Duflos C, et al. **Hemophagocytic lymphohistiocytosis gene mutations in adult patients presenting with CLIPPERS-like syndrome.** *Neurol Neuroimmunol Neuroinflamm* 2021;8:e970 CrossRef Medline

29. Chiapparini L, Uziel G, Vallinoto C, et al. **Hemophagocytic lymphohistiocytosis with neurological presentation: MRI findings and a nearly miss diagnosis.** *Neurol Sci* 2011;32:473–77 CrossRef Medline

30. Gray PE, Shadur B, Russell S, et al. **Late-onset non-HLH presentations of growth arrest, inflammatory arachnoiditis, and severe infectious mononucleosis, in siblings with hypomorphic defects in UNC13D.** *Front Immunol* 2017;8:944.CrossRef Medline

31. Trizzino A, Stadt U. Z, Ueda I, et al; Histiocyte Society HLH Study group. **Genotype-phenotype study of familial haemophagocytic lymphohistiocytosis due to perforin mutations.** *J Med Genet* 2007;45:15–21 CrossRef Medline